

Formation of a “Cluster Molecule” $(C_{20})_2$ and Its Thermal Stability

A. I. Podlivaev and L. A. Openov*

Moscow Engineering Physics Institute (State University), 115409 Moscow, Russia

* E-mail: LAOpenov@mephi.ru

ABSTRACT

The possible formation of a “cluster molecule” $(C_{20})_2$ from two single C_{20} fullerenes is studied by the tight-binding method. Several $(C_{20})_2$ isomers in which C_{20} fullerenes are bound by strong covalent forces and retain their identity are found; actually, these C_{20} fullerenes play the role of “atoms” in the “cluster molecule”. The so-called *open*-[2+2] isomer has a minimum energy. Its formation path and thermal stability at $T = 2000 \div 4000$ K are analyzed in detail. This isomer loses its molecular structure due to either the decay of one of C_{20} fullerenes or the coalescence of two C_{20} fullerenes into a C_{40} cluster. The energy barriers for the metastable *open*-[2+2] configuration are calculated to be $U = 2 \div 5$ eV.

1. INTRODUCTION

The discovery of fullerene C_{60} [1] stimulated extensive theoretical and experimental studies of carbon clusters and other carbon nanostructures. In 2000, the fullerene C_{20} that is the smallest among all possible fullerenes was detected (Fig. 1): on its surface, C-C bonds form only regular pentagons and there are no hexagons (unlike in C_n fullerenes with $n > 20$) [2]. Later, the authors of [3] obtained experimental evidence for the charged cluster dimers and $(C_{20})_k^+$ with $k = 3 \div 13$. In the future, it would be interesting to synthesize a macroscopic C_{20} -fullerene-based cluster matter (by analogy with a fullerite made of C_{60} clusters [4]). According to theoretical studies [5-7], such a matter can be a superconductor with an extremely high critical temperature.

An analysis of the paths of formation of the C_{20} fullerite should begin with a detailed discussion of C_{20} cluster dimerization. The structural and energetic characteristics of $(C_{20})_2$ dimers were first studied theoretically in [5] (by the density functional method in the local-density approximation with gradient corrections) and in [8] (by the Hartree-Fock and density functional methods with the B3LYP exchange-correlation functional). The authors of [8] found several metastable $(C_{20})_2$ isomers with different number, strength, and length of intercluster bonds. Three of them are shown in Fig. 2. The *open*-[2+2] isomer has a minimum energy (Fig. 2c); hereafter numerals in square brackets mean the number of atoms of each fullerene involved in the intercluster bonding. As was shown in [8], when the *open*-[2+2] isomer forms, the energy of the $(C_{20})_2$ system remains below the total energy of two single C_{20} fullerenes approaching each other; that is, the open *open*-[2+2] configuration is favorable from both the kinetic and thermodynamic viewpoint.

In this work, the path of formation of a “cluster molecule” $(C_{20})_2$ from two C_{20} fullerenes

is studied using the tight-binding potential [9]. We analyze the potential-energy surfaces at various sections of this path and find the energy barriers that hinder the loss of molecular structure of the $(C_{20})_2$ dimer. Using molecular dynamics simulation, we investigate the evolution of the $(C_{20})_2$ dimer in real time at temperatures high enough to overcome the barriers. The results obtained indicate that the *open*-[2+2] isomer is rather stable.

2. COMPUTATIONAL PROCEDURE

We calculate the potential energy of the $(C_{20})_2$ system by the tight-binding method with the transferable interatomic potential [9] in the Born-Oppenheimer approximation at fixed coordinates $\{\mathbf{R}_i\}$ of all atoms ($i = 1 - 40$ is the atom number). This method is a reasonable compromise between oversimplified classical approaches and *ab initio* calculations requiring much computational time. Earlier [10-14], we used this method to simulate various carbon clusters, including C_{60} and C_{20} fullerenes. The energy $E_{pot}(\{\mathbf{R}_i\})$ is equal to the sum of the classical atomic repulsion energy and the so-called band energy, which can be found by diagonalizing the Hamiltonian matrix in the site representation and by summation the energies of one-electron levels occupied according to the Pauli principle [9]. We took into account the valence electrons occupying the $2s$, $2p_x$, $2p_y$, and $2p_z$ orbitals of each carbon atom. The interatomic distances, binding energies, HOMO-LUMO gaps, and other characteristics calculated for C_{60} and C_{20} clusters using this method agree with the experimental data and the results of *ab initio* calculations [13, 14].

The forces \mathbf{F}_i acting on atoms were determined from the Hellmann-Feynman formula by calculating the matrix elements of the gradient of the tight-binding Hamiltonian between occupied eigenstates. The temperature T_{el} of the electron subsystem was taken to be zero, which simplifies the calculations. We chose this approximation due to the following reasons:

first, the results of molecular dynamics for a single C_{20} fullerene at $T_{el} = 0$ and 3000 K differ only slightly [13] and, second, in the $(C_{20})_2$ dimer, the HOMO-LUMO gap separating the upper unoccupied one-electron orbitals from the lower occupied ones is larger than that in the C_{20} fullerene (0.65 and 0.43 eV, respectively). As a result, excited electron states are less significant in the temperature range under study.

To study the evolution of the $(C_{20})_2$ dimer at high temperatures, we performed molecular-dynamics simulation with the tight-binding potential used in [9] and a time step $t_0 = 2.72 \cdot 10^{-16}$ s. The total energy of the system (the sum of the potential and kinetic energies) remained unchanged during simulation, and the system temperature T was determined from the formula

$$\frac{1}{2}k_B T(3n - 6) = \langle E_{\text{kin}} \rangle, \quad (1)$$

where k_B is the Boltzmann constant, $n = 40$ is the number of atoms in the system, and $\langle E_{\text{kin}} \rangle$ is the time-averaged kinetic energy. This formulation of the problem corresponds to the situation where the system is not in thermal equilibrium with its environment. The microcanonical temperature T is a measure of the energy of relative atomic motion [15]. At the initial time, all atoms were given random velocities and displacements such that the momentum and the angular momentum of the system were zero. Then, we calculated the forces acting on atoms and numerically solved the classical Newton equations of motion.

To analyze the potential-energy surfaces $E_{\text{pot}}(\{\mathbf{R}_i\})$, to determine the paths of the system between various states, and to find the heights U of the energy barriers present in these paths, we performed structure relaxation and found the saddle points of the energy $E_{\text{pot}}(\{\mathbf{R}_i\})$ as a function of the normal coordinates corresponding to unstable atomic equilibrium [13].

3. FORMATION OF THE $(C_{20})_2$ DIMER

As in [8], we found several metastable configurations $(C_{20})_2$. Three of them, including the *open*-[2 + 2] isomer (which has a minimum energy), are shown in Fig. 2. The binding energies E_b of these isomers were calculated from the formula

$$E_b = E_{\text{pot}}(C_1) - E_{\text{pot}}(C_n) / n, \quad (2)$$

where n is the number of atoms in the system ($n = 40$ for the $(C_{20})_2$ dimer), $E_{\text{pot}}(C_1)$ is the energy of a single carbon atom, and $E_{\text{pot}}(C_n)$ is the energy of an n -atom configuration. The binding energies were calculated to be 6.14, 6.16, and 6.20 eV/atom for the [1 + 1], [2 + 2], and *open*-[2 + 2] isomers, respectively. All of these values of E_b are higher than the binding energy of one C_{20} fullerene ($E_b = 6.08$ eV/atom) calculated by the same tight-binding method [13]. Therefore, the energy E_{pot} of these isomers is lower than the total energy of two single C_{20} fullerenes; that is, their formation is favorable from a thermodynamic viewpoint. The coalescence energies $\Delta E = 2E_{\text{pot}}[C_{20}] - E_{\text{pot}}[(C_{20})_2]$ for the [1 + 1], [2 + 2], and *open*-[2 + 2] isomers are 2.5, 3.2, and 4.9 eV, respectively. The values of ΔE calculated by the Hartree-Fock and density functional methods are 2.3, 5.9, and 7.1 eV and 2.4, 4.7, and 6.3 eV, respectively [8]. It is seen that, although the absolute values of ΔE differ quite significantly, different theoretical approaches result in the same sequence of $(C_{20})_2$ isomers from an energetic viewpoint. The validity of our potential is also supported by the fact that the bond lengths in $(C_{20})_2$ dimers agree well with the data from [8] (see Fig. 2).

An analysis of the potential energy E_{pot} as a function of the atomic coordinates $\{\mathbf{R}_i\}$ demonstrates that there is no barrier in the path of formation of the [1 + 1] isomer from two C_{20} fullerenes (Fig. 3a). As a result of the coalescence of two fullerenes, a $(C_{20})_2$ dimer with one 1-2 bond forms (numerals indicate the atom numbers; see Fig. 2). In turn, the [1 + 1]

isomer can transform into a $[2 + 2]$ isomer, which has a lower energy, by overcoming a barrier $U = 0.33$ eV (Fig. 3b). In this case, the C_{20} fullerenes rotate about the 1-2 bond with respect to each other, which leads to the formation of a second (3-4) bond between them. The barrier height for the $[2 + 2]$ isomer to transform into the *open*- $[2 + 2]$ isomer (Fig. 2c), which has a minimum energy, is $U = 0.57$ eV (Fig. 3c). This transition proceeds via the sequential breaking of intracuster 1-3 and 2-4 bonds.

Our results are in overall agreement with the results of [8] except for the fact that the authors of [8] failed to determine the barrier height in the $[1 + 1] \rightarrow [2 + 2]$ path because of the small curvature of the potential surface in the vicinity of the $[1 + 1]$ configuration. Nevertheless, we confirmed the main conclusion drawn in [8] that, along the entire path of the $C_{20} + C_{20} \rightarrow [1 + 1] \rightarrow [2 + 2] \rightarrow \textit{open}$ - $[2 + 2]$ transition (including saddle points), the energy of the system remains below the total energy of two C_{20} fullerenes located far from each other (Fig. 3). Hence, the formation of the *open*- $[2 + 2]$ isomer does not require energy consumption and is favorable from both the thermodynamic and kinetic viewpoint.

4. STABILITY OF THE $(C_{20})_2$ DIMER

Although the *open*- $[2 + 2]$ isomer has the maximum binding energy among all $(C_{20})_2$ dimers, this isomer should be considered a metastable configuration of 40 carbon atoms. Indeed, although E_b for the *open*- $[2 + 2]$ isomer is 0.12 eV/atom higher than that of two single C_{20} fullerenes, it is 0.35 eV/atom lower than that of fullerene C_{40} . Therefore, it is energetically favorable for the $(C_{20})_2$ dimer to lose its molecular structure via the coalescence of its two C_{20} clusters into one large C_{40} fullerene, by analogy with the synthesis of light nuclei [16]. In order to study the stability of the C_{20} dimer against this transformation, one should determine the energy barrier U that hinders this coalescence.

Our numerical simulation of the dynamics of the *open*-[2 + 2] isomer at $T = 2000 \div 4000$ K indicates that it does lose its molecular structure (in which its two C_{20} clusters retain their identity). The average time τ of such a loss ranges from 1 ps to 10 ns depending on the temperature T . However, we found that the C_{40} fullerene is not formed in this case but rather various C_{40} clusters appear with a binding energy lower than that of the 40-atom fullerene (but higher than that of the *open*-[2 + 2] isomer).

The shape of the C_{40} cluster that forms most often is shown in Fig. 4a. At first glance, it forms via the rotation of one C_{20} - C_{20} bond through 90° (as in the Stone-Wales transformation in fullerene C_{60} [17]). However, analysis demonstrates that the character of the rearrangement of the C-C bonds is more complex. After the 1-5 and 4-6 bonds (which are intraccluster bonds for the C_{20} fullerenes in the $(C_{20})_2$ dimer) have been broken (Fig. 2c), new bonds (1-4, 5-6) appear. Atoms 1 and 4, which belonged earlier to different C_{20} fullerenes, are “collectivized”, and 1-4 bond becomes an intraccluster bond for the C_{40} cluster. The binding energy of this cluster is $E_b = 6.25$ eV/atom, which is 0.05 eV/atom higher than that of the *open*-[2 + 2] isomer. This cluster can be considered as a defect isomer of the C_{40} fullerene whose surface contains two nonagons apart from pentagons and hexagons. Recall that, in the C_{40} fullerene, the C-C bonds between the nearest carbon atoms form twelve pentagons and ten hexagons.

To find the energy barrier U that hinders the transformation of the $(C_{20})_2$ dimer into the C_{40} cluster shown in Fig. 4a, we calculated the potential relief $E_{\text{pot}}(\{\mathbf{R}_i\})$ in the vicinity of the *open*-[2 + 2] metastable state (Fig. 5). Thus, we found $U = 2.5$ eV and determined the atomic configurations of two transient atomic states corresponding to the saddle points of $E_{\text{pot}}(\{\mathbf{R}_i\})$ and the atomic configuration of an intermediate metastable state corresponding to a local minimum of $E_{\text{pot}}(\{\mathbf{R}_i\})$. In the intermediate state (Fig. 4b), another bond appears

between the C_{20} fullerenes; the midpoint of this bond is the center of symmetry of this atomic configuration. The intermediate state is separated from the *open*-[2 + 2] isomer by a relatively low barrier ($U = 0.63$ eV) and is located in a relatively flat section of the potential energy surface. Therefore, numerous configurations with energies close to the intermediate-state energy can exist; the $(C_{20})_2$ dimer can easily transform into these configurations by passing through barrier 2 and stay in these states for a long time until it coalesces to form the C_{40} cluster. This behavior is supported by the molecular dynamics data.

We also observed the coalescence of C_{20} fullerenes into other C_{40} clusters; some of them (after relaxation) are depicted in Fig. 6. The binding energy of one of these clusters (Fig. 6a) is $E_b = 6.195$ eV/atom, which is close to that of the *open*-[2 + 2] isomer (the former energy is even slightly lower); that is, the transition occurs between two almost energetically degenerate configurations. The surface of this cluster has one eight-member and two ten-member “windows”. The binding energies of the other C_{40} clusters are significantly higher than that of the *open*-[2 + 2] isomer. The value of E_b is the higher, the smaller the number of N -gons with $N \geq 7$ in the cluster and/or the smaller the number of atoms N in them (i.e., the closer the structure of the cluster to the C_{40} fullerene). For example, $E_b = 6.32$ eV/atom in a C_{40} cluster with two octagons (Fig. 6b), $E_b = 6.36$ eV/atom in a C_{40} cluster with one octagon and one heptagon (Fig. 6c), and $E_b = 6.49$ eV/atom in a C_{40} cluster with one heptagon (Fig. 6d). We also observed transformations of the $(C_{20})_2$ dimer into C_{40} clusters having one octagon and two heptagons ($E_b = 6.34$ eV/atom), four heptagons ($E_b = 6.35$ eV/atom), and so on. All these clusters are so-called nonclassical C_{40} fullerene isomers, since, apart from pentagons and hexagons, they contain at least one N -gon with $N \geq 7$ [18].

An analysis of the shape of the potential energy surface shows that the heights of the

energy barriers to the transitions of the $(C_{20})_2$ dimer into C_{40} clusters of different types differ substantially; in most cases, we have $U = 2 \div 4$ eV. When simulating the evolution of the $(C_{20})_2$ dimer, we assumed that the total energy of the system is constant. As a result, the formation of a C_{40} cluster with a binding energy E_b higher than that of the $(C_{20})_2$ dimer (i.e., with a lower potential energy E_{pot}) is accompanied by heating of the cluster. This leads to the annealing of defects (N -gons with $N \geq 7$) and sequential transitions of the C_{40} cluster into configurations with a progressively higher binding energy. However, the system temperature also increases. As a result, the C_{40} cluster decomposes, i.e., loses its spherical shape and transforms into quasi-one-dimensional or quasi-twodimensional configurations. Although this decomposition is unfavorable from a thermodynamic viewpoint (since it increases the potential energy), it is, nevertheless, irreversible. This is related to the presence of numerous low-dimensional configurations with close energies into which the C_{40} cluster transforms sequentially after decomposition. The number of such configurations that are geometrically close to the fullerene and can transform into it is very small. Therefore, the process of decomposition is irreversible despite the high potential energy of the decomposed cluster and the relatively low energy barrier separating the atomic configurations appearing after decomposition from the compact fullerene. A similar situation was detected in the simulation of the thermal stability of the C_{20} fullerene [13]. Note that we did not observe the reverse transformation from the C_{40} cluster into the $(C_{20})_2$ dimer.

The $(C_{20})_2$ dimer loses its molecular structure not only through the coalescence of two C_{20} fullerenes into a C_{40} cluster. We also observed another scenario of stability loss of the *open*-[2 + 2] isomer. At a high temperature, only one of the C_{20} fullerenes forming the $(C_{20})_2$ dimer can decompose, while the other C_{20} fullerene retains its shape. Figure 7 shows the

typical atomic configuration formed upon this decomposition. Its binding energy ($E_b = 6.14$ eV/atom) is lower than that of the $(C_{20})_2$ dimer. Therefore, the decay of one C_{20} fullerene is accompanied by an increase in the potential energy E_{pot} and, hence, by cooling of the cluster. The reverse transformation of the system into the $(C_{20})_2$ dimer does not occur for the reasons discussed above.

An analysis of the molecular dynamics data reveals that the decay of one C_{20} fullerene in the $(C_{20})_2$ dimer can proceed in different ways, see [19] for more details. Figure 8 shows the dependence of the potential energy E_{pot} on the reaction coordinate X for one of the decay channels. The sequence of the breaking of interatomic bonds is identical to that for the decomposition of a single C_{20} fullerene [13]: first, two C-C bonds are broken simultaneously and two adjacent octagons form on the “lateral surface” and, then, three more C-C bonds are sequentially broken. As a result, the number of octagons on the lateral surface increases to five and, finally, the defect C_{20} fullerene decomposes (Fig. 7). The barrier height is $U = 5.0$ eV, as in the case of a single C_{20} fullerene (Fig. 8). However, there are two differences: (i) $E_{pot}(X)$ reaches a maximum as the fifth rather than the fourth C-C bond is broken, and (ii) the atomic configuration with two broken C-C bonds is not metastable. Although there exist other channels of decomposition of one C_{20} fullerene in the $(C_{20})_2$ dimer (they are characterized by $U = 3 \div 5$ eV), the decomposition usually begins with the breakage of two C-C bonds, as in the case described above.

The energy barrier to the coalescence of two C_{20} fullerenes into a C_{40} cluster ($U = 2 \div 4$ eV) is somewhat lower than the barrier to the decomposition of one C_{20} fullerene ($U = 3 \div 5$ eV). Therefore, as the temperature decreases, the former mechanism of stability loss in the $(C_{20})_2$ dimer becomes more important. It should be noted, however, that there are cases

that a clear distinction between these two decay channels cannot be made. For example, we observed a situation in which a C_{40} cluster formed before the decomposition of one C_{20} fullerene was completed. In another case, in contrast, a C_{40} cluster existed only for a short time (less than 1 ps) and then decomposed in such a manner that only one of its halves transformed into a low-dimensional configuration, whereas the other half retained the shape of the C_{20} fullerene. The latter scenario occurred primarily when the C_{40} cluster formed at the first stage was a defect C_{40} fullerene isomer similar to that shown in Fig. 6a. With these exceptions, the character of the molecular structure loss of the $(C_{20})_2$ dimer (i.e., coalescence or decomposition) is determined unambiguously.

5. CONCLUSIONS

In this study, we have shown that there is no energy barrier to the formation of a $(C_{20})_2$ cluster dimer from two single C_{20} fullerenes; that is, the formation of this dimer (*open*-[2 + 2] isomer) is favorable from both the kinetic and thermodynamic viewpoint. This result was obtained by the tight-binding method and supplements the data obtained earlier [8] using the Hartree-Fock and density functional methods.

The barriers that hinder the molecular structure loss of the $(C_{20})_2$ dimer are $U = 2 \div 4$ eV for the coalescence of two C_{20} fullerenes into a C_{40} cluster and $U = 3 \div 5$ eV for the decomposition of one C_{20} fullerene in the $(C_{20})_2$ dimer. Thus, although the stability of the $(C_{20})_2$ dimer is lower than that of the C_{20} fullerene (for which $U = 5$ eV), it is rather high. In the near future, it would be interesting to study and simulate the potential energy surfaces and dynamics of the C_{20} -fullerene-based three-dimensional structures discussed in the literature, determine their stability, and calculate the formation energies of various structural defects.

References

- [1] H.W. Kroto, J.R. Heath, S.C. O'Brien, R.F. Curl, R.E. Smalley, *Nature* **318**, 162 (1985).
- [2] H. Prinzbach, A. Weller, P. Landenberger, F. Wahl, J. Worth, L.T. Scott, M. Gelmont, D. Olevano, B. von Issendorff, *Nature* **407**, 60 (2000).
- [3] R. Ehlich, P. Landenberger, H. Prinzbach, *J. Chem. Phys.* **115**, 5830 (2001).
- [4] A.V. Eletskii, B.M. Smirnov, *Usp. Fiz. Nauk* **165**, 977 (1995) [*Phys. Usp.* **38**, 935 (1995)].
- [5] Y. Miyamoto, M. Saito, *Phys. Rev. B* **63**, 161401 (2001).
- [6] S. Okada, Y. Miyamoto, M. Saito, *Phys. Rev. B* **64**, 245405 (2001).
- [7] I. Spagnolatti, M. Bernasconi, G. Benedek, *Europhys. Lett.* **59**, 572 (2002).
- [8] C.H. Choi, H.-I. Lee, *Chem. Phys. Lett.* **359**, 446 (2002).
- [9] C.H. Xu, C.Z. Wang, C.T. Chan, K.M. Ho, *J. Phys.: Condens. Matter* **4**, 6047 (1992).
- [10] L.A. Openov, V.F. Elesin, *Pis'ma Zh. Eksp. Teor. Fiz.* **68**, 695 (1998) [*JETP Lett.* **68**, 726 (1998)]; physics/9811023.
- [11] V.F. Elesin, A.I. Podlivaev, L.A. Openov, *Phys. Low-Dim. Struct.* **11/12**, 91 (2000); physics/0104058.
- [12] N.N. Degtyarenko, V.F. Elesin, N.E. L'vov, L.A. Openov, A.I. Podlivaev, *Fiz. Tverd. Tela (St. Petersburg)* **45**, 954 (2003) [*Phys. Solid State* **45**, 1002 (2003)].
- [13] I.V. Davydov, A.I. Podlivaev, L.A. Openov, *Fiz. Tverd. Tela (St. Petersburg)* **47**, 751 (2005) [*Phys. Solid State* **47**, 778 (2005)]; cond-mat/0503500.

- [14] A.I. Podlivaev, L.A. Openov, Pis'ma Zh. Eksp. Teor. Fiz. **81**, 656 (2005) [JETP Lett. **81**, 533 (2005)]; cond-mat/0506571.
- [15] C. Xu, G.E. Scuseria, Phys. Rev. Lett. **72**, 669 (1994).
- [16] V.F. Elesin, N.N. Degtyarenko, L.A. Openov, Inzh. Fiz. **3**, 2 (2002), in Russian.
- [17] A.J. Stone, D.J. Wales, Chem. Phys. Lett. **128**, 501 (1986).
- [18] E. Hernández, P. Ordejón, H. Terrones, Phys. Rev. B **63**, 193403 (2001).
- [19] L.A. Openov, A.I. Podlivaev, cond-mat/0610033.

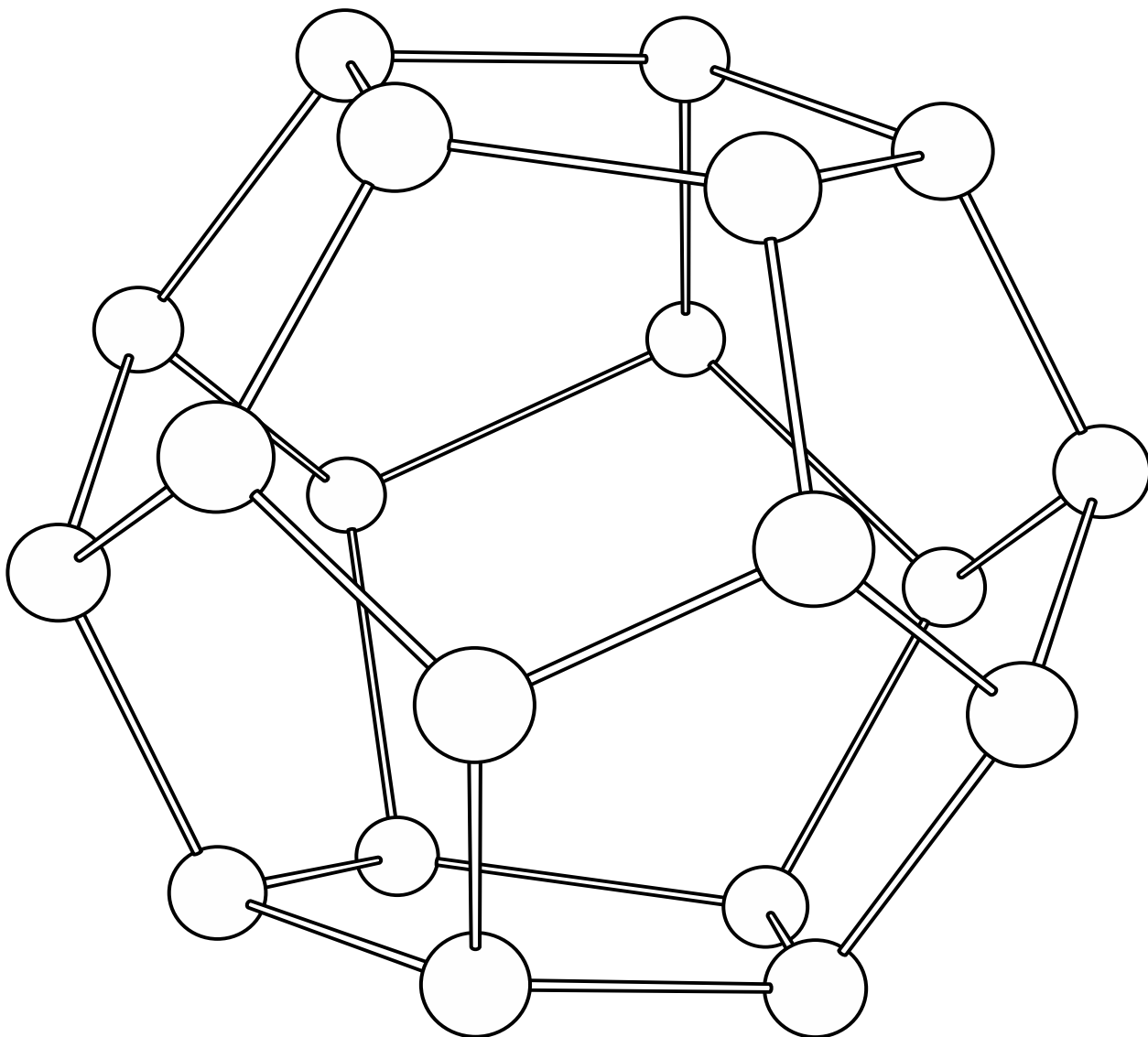


Fig. 1. Fullerene C₂₀. The binding energy is $E_b = 6.08$ eV/atom.

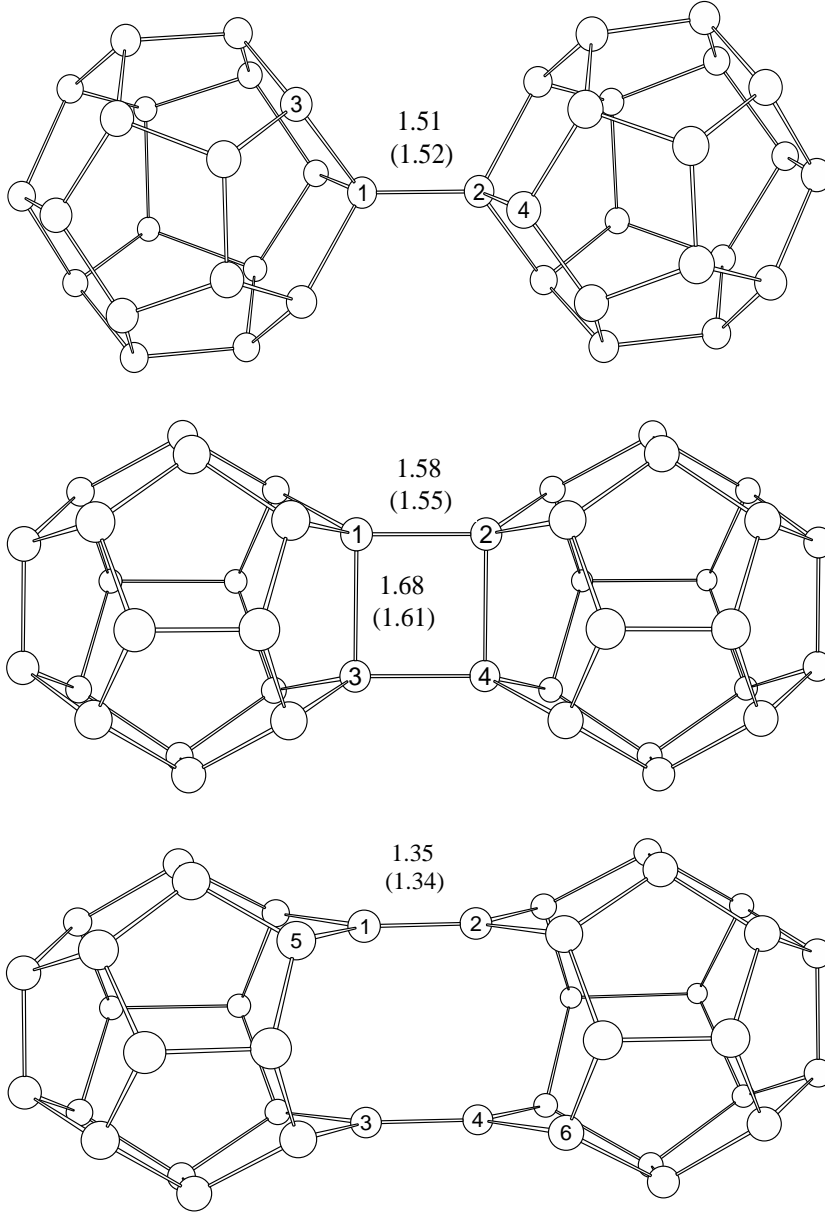


Fig. 2. Isomers $(C_{20})_2$: (a) $[1+1]$ with a binding energy $E_b = 6.14$ eV/atom, (b) $[2+2]$ with a binding energy $E_b = 6.16$ eV/atom, and (c) *open*- $[2+2]$ with a binding energy $E_b = 6.20$ eV/atom. The numerals above parentheses indicate the bond lengths in angstroms, and the numerals in parentheses are the bond lengths calculated in [8] using the density functional method.

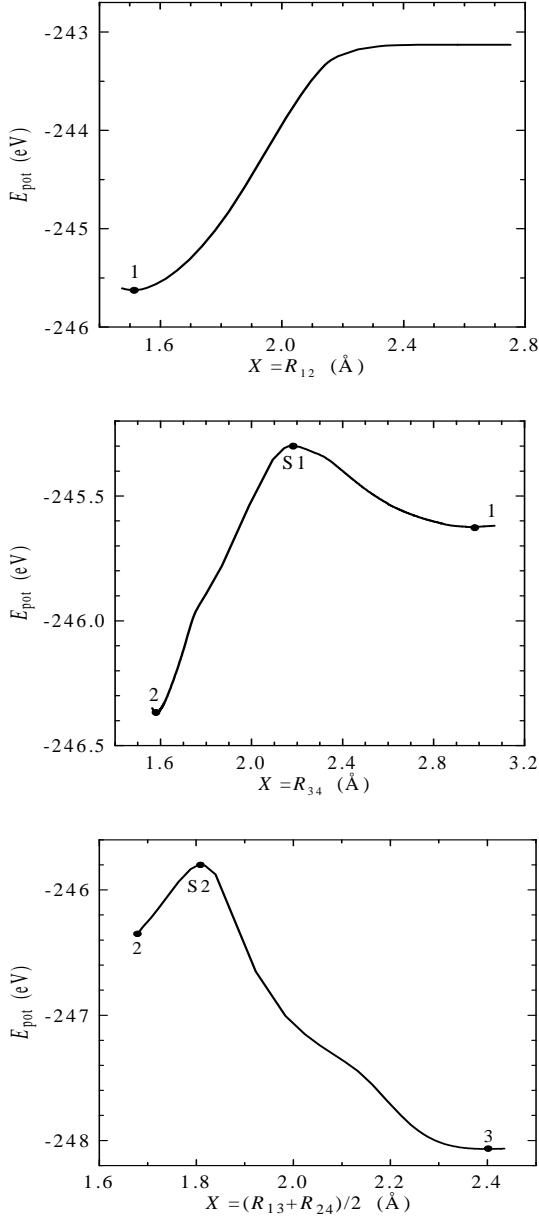


Fig. 3. Dependence of the potential energy E_{pot} of the $(\text{C}_{20})_2$ dimer on the reaction coordinate X for (a) the $\text{C}_{20} + \text{C}_{20} \rightarrow [1 + 1]$, (b) $[1 + 1] \rightarrow [2 + 2]$, and (c) $[2 + 2] \rightarrow \text{open-[2 + 2]}$ transitions. Points in curves correspond to (1) the $[1 + 1]$ isomer, (2) $[2 + 2]$ isomer, and (3) *open*- $[2 + 2]$ isomer. S1 and S2 are the $E_{\text{pot}}(X)$ maxima, i.e., saddle points in $E_{\text{pot}}(\{\mathbf{R}_i\})$. The reference point was taken to be the energy of 40 isolated carbon atoms. The X coordinates are chosen in terms of interatomic distances (see Fig. 2).

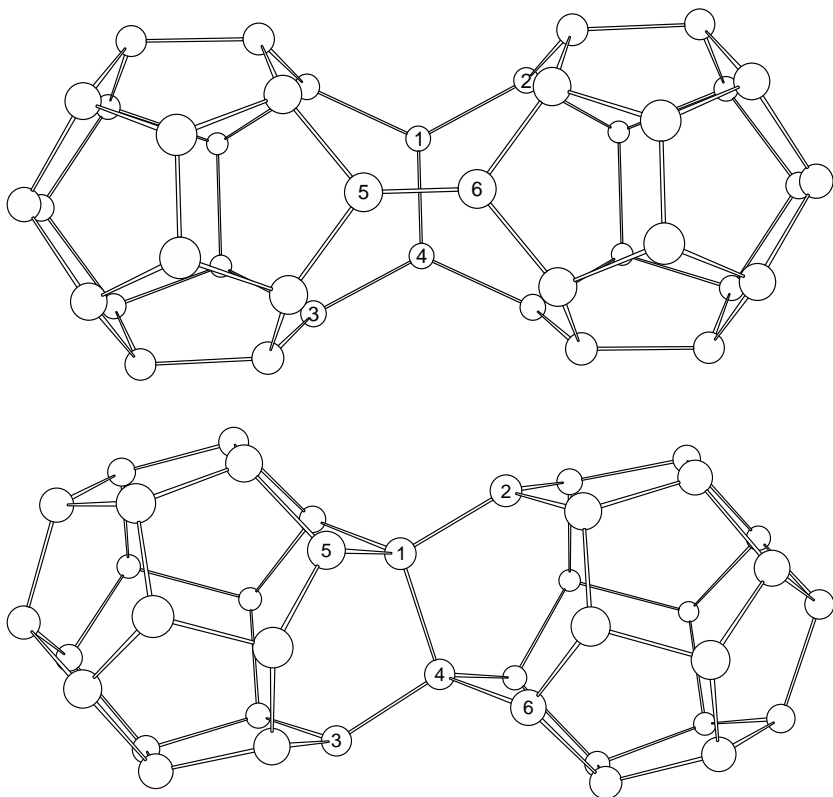


Fig. 4. (a) One of the C_{40} clusters formed upon the coalescence of the C_{20} fullerenes in the $(C_{20})_2$ dimer. The binding energy is $E_b = 6.25$ eV/atom. (b) The intermediate metastable state that forms when the *open*-[2 + 2] isomer transforms into a C_{40} cluster (see Fig. 5). $E_b = 6.19$ eV/atom. The numbering of atoms is identical to that in Fig. 2c.

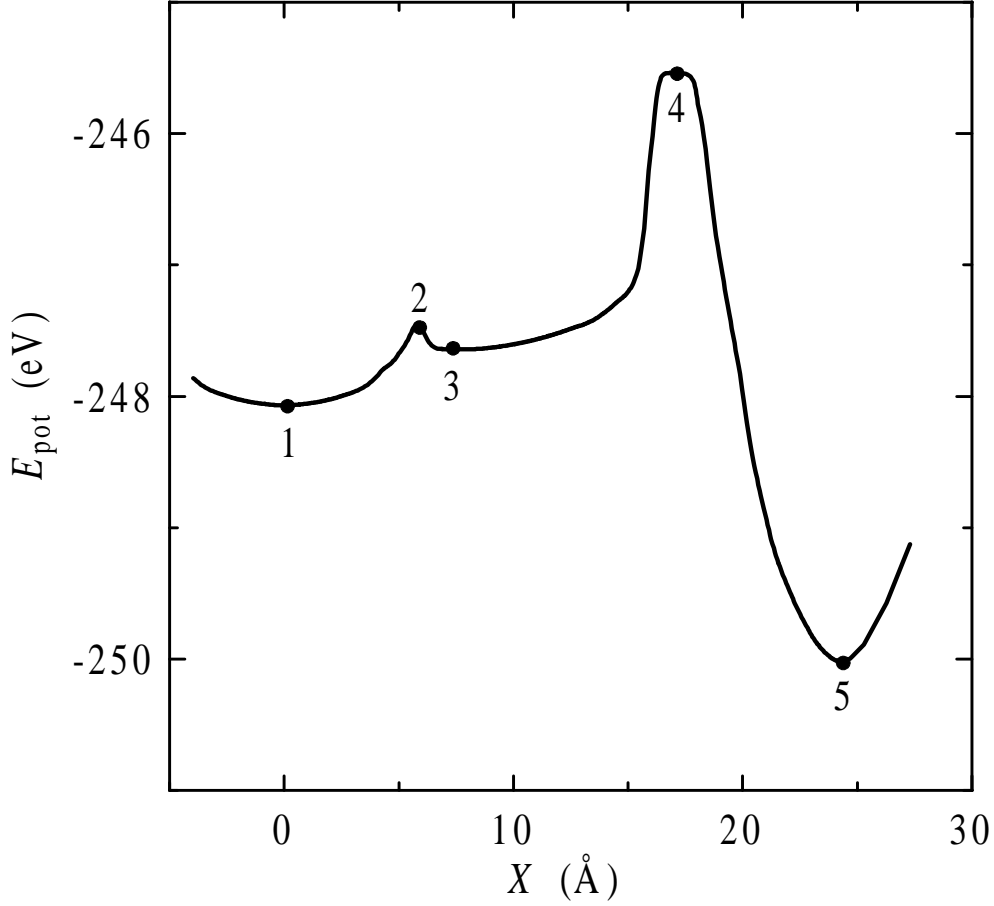


Fig. 5. Dependence of the potential energy E_{pot} of the $(\text{C}_{20})_2$ dimer on the reaction coordinate X for the transformation of the *open*-[2 + 2] isomer into the C_{40} cluster shown in Fig. 4a. Points in the curve indicate (1) the *open*-[2 + 2] isomer; (2, 4) local maxima in $E_{\text{pot}}(X)$, i.e. saddle points for $E_{\text{pot}}(\{\mathbf{R}_i\})$; (3) the local minimum in $E_{\text{pot}}(X)$ corresponding to the metastable intermediate state shown in Fig. 4b; and (5) a C_{40} cluster (Fig. 4a). The reference point is taken to be the energy of 40 isolated carbon atoms. The reaction coordinate is chosen to be the length of the path that passes through the corresponding saddle point in the $(3n - 6)$ -dimensional space and connects the *open*-[2 + 2] isomer and the C_{40} cluster (as in [14]).

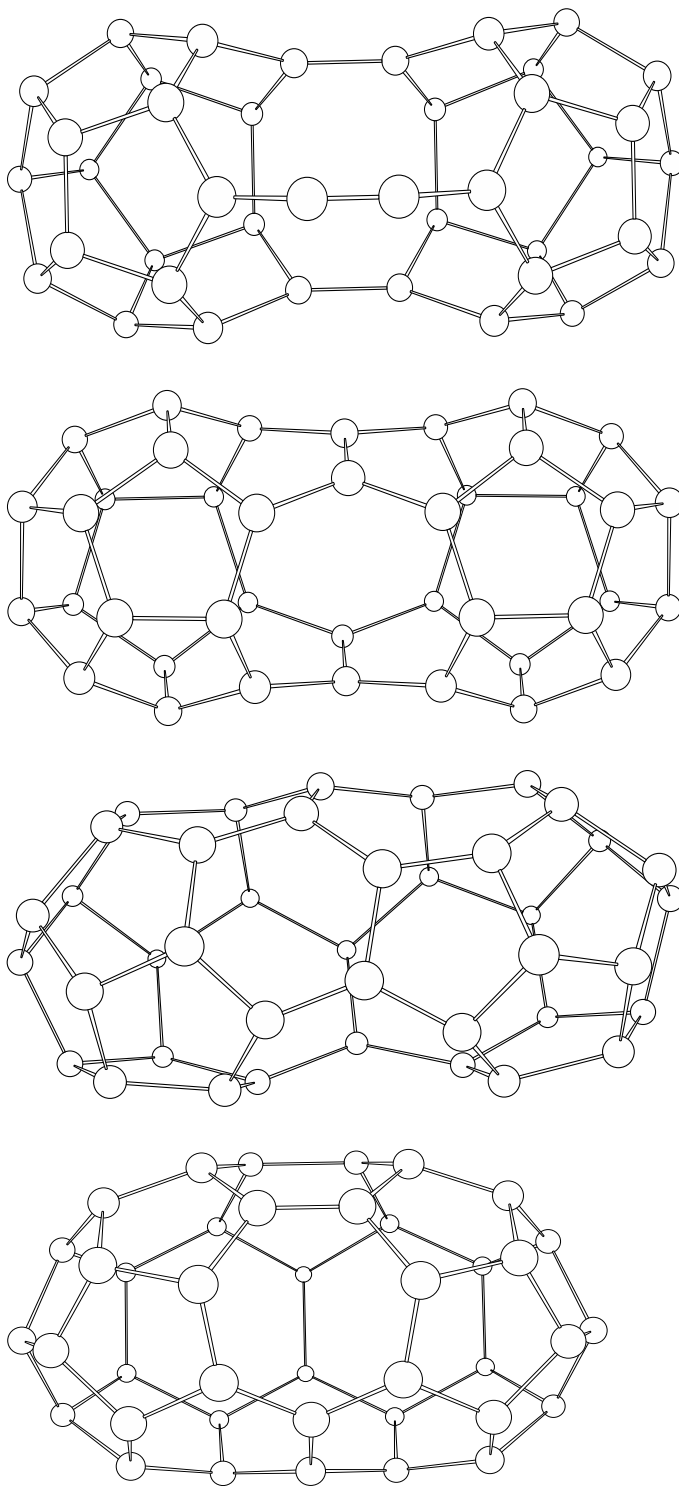


Fig. 6. Some of the C_{40} clusters formed from the $(C_{20})_2$ dimer at a high temperature. Their binding energies E_b (after relaxation) are (a) 6.195, (b) 6.32, (c) 6.36, and (d) 6.49 eV/atom.

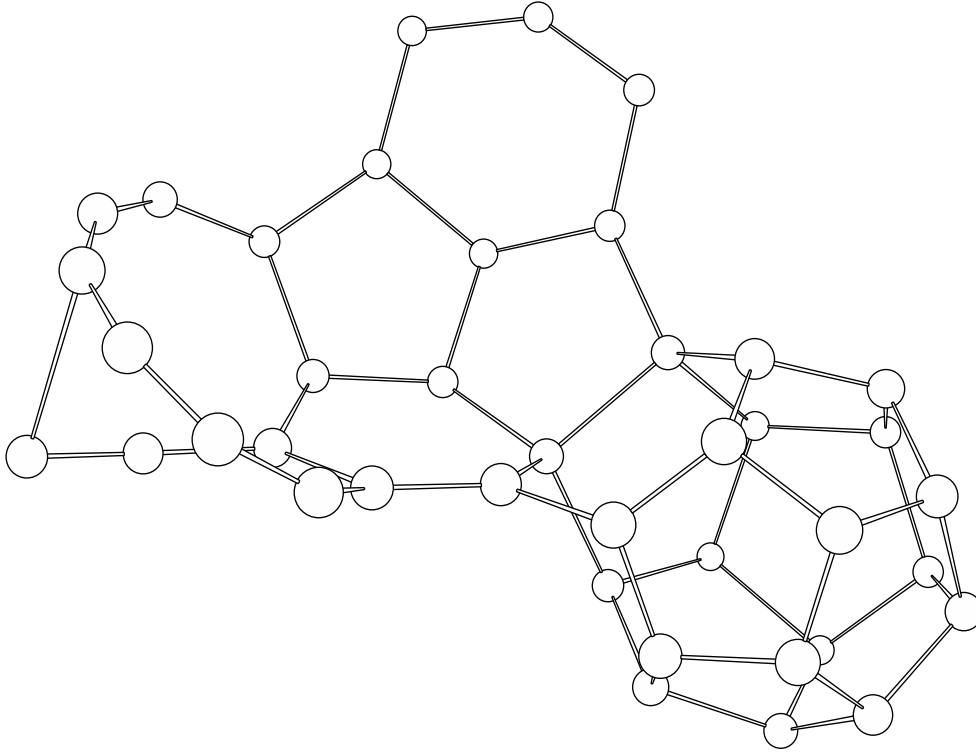


Fig. 7. Atomic configuration after the decomposition of one C_{20} fullerene in the $(C_{20})_2$ dimer. The binding energy is $E_b = 6.14$ eV/atom.

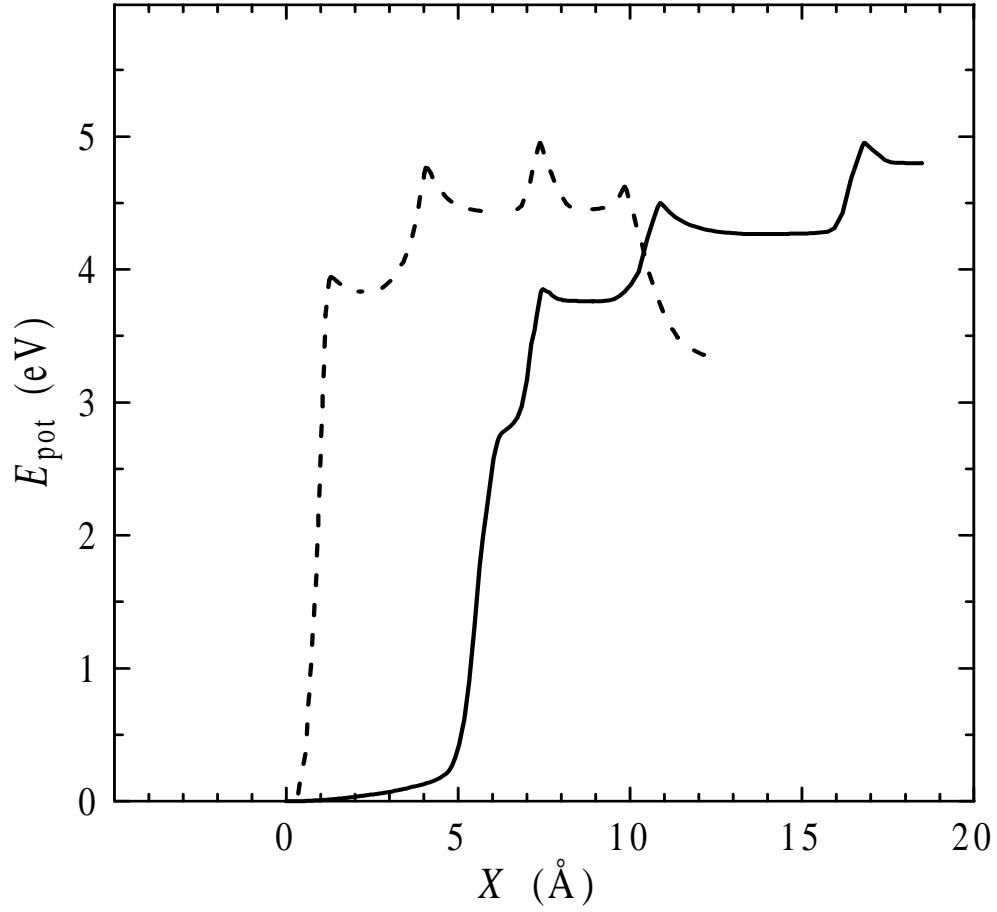


Fig. 8. Dependence of the potential energy E_{pot} of the $(C_{20})_2$ dimer on the reaction coordinate X for the decay of one C_{20} fullerene in the $(C_{20})_2$ dimer (solid line) and for the decay of a single C_{20} fullerene (dashed line). The reference point is taken to be the energy of the *open*-[2 + 2] isomer and the C_{20} fullerene, respectively. The reaction coordinate X is the same as in Fig. 5.